Inorg. Chem. **2005**, *44*, 3524–3536

Syntheses, Structures, and Magnetic Properties of Diphenoxo-Bridged $M^{II}Ln^{III}$ Complexes Derived from *N,N′*-Ethylenebis(3-ethoxysalicylaldiimine) (M = Cu or Ni; Ln = Ce–Yb): Observation of Surprisingly Strong Exchange Interactions

Rajesh Koner,[†] Hsin-Huang Lin,[‡] Ho-Hsiang Wei,*[,‡] and Sasankasekhar Mohanta*[,†]

Departments of Chemistry, University of Calcutta, 92 A. P. C. Ray Road, Kolkata 700 009, India, and Tamkang University, Tamsui, Taiwan 25137

Received December 21, 2004

A series of heterodinuclear $Cu^{II}Ln^{III}$ and $Ni^{II}Ln^{III}$ complexes, $[M^{II}L^{1}Ln^{III}(NO_3)_3]$ (M = Cu or Ni; Ln = Ce–Yb), with the hexadentate Schiff base compartmental ligand *N,N′*-ethylenebis(3-ethoxysalicylaldiimine) (H_2L^1) have been synthesized and characterized. The X-ray crystal structure determinations of 13 of these compounds reveal that they are all isostructural. All of these complexes crystallize with the same orthorhombic $P2_12_12_1$ space group with closely similar unit cell parameters. Typically, the structure consists of a diphenoxo-bridged 3d–4f dinuclear core, self-assembled to two dimensions due to the intermolecular nitrate···copper(II) or nitrate···nickel(II) semicoordination and weak C–H···O hydrogen bonds. Despite that, the metal centers of the neighboring units are well separated (the ranges of the shortest intermolecular contacts (Å) are (M···M) 7.46–7.60, (Ln···Ln) 8.56–8.69, and (M···Ln) 6.12–6.20). Variable-temperature (5–300 K) magnetic susceptibility measurements of all the complexes have been made. The nature of exchange interactions in the $Cu^{II}Ln^{III}$ systems has been inferred from the $\Delta\chi_M T$ versus T plots, where $\Delta\chi_M T$ is the difference between the values of $\chi_M T$ for a $Cu^{II}Ln^{III}$ system and its corresponding $Ni^{II}Ln^{III}$ analogue. Ferromagnetic interactions seem to be exhibited by the $Cu^{II}Gd^{III}$, $Cu^{II}Tb^{III}$, $Cu^{II}Dy^{III}$, $Cu^{II}Ho^{III}$, $Cu^{II}Tm^{III}$, and $Cu^{II}Yb^{III}$ complexes, while, for the $Cu^{II}Er^{III}$ complex, no definite conclusion could be reached. On the other hand, among the lower members of the series, the complexes of Ce^{III}, Nd^{III}, and Sm^{III} exhibit antiferromagnetic interactions, while the $Cu^{II}Pr^{III}$ and $Cu^{II}Eu^{III}$ analogues behave as spin-uncorrelated systems. The observations made here vindicate the proposition of Kahn (*Inorg. Chem.* **1997**, *36*, 930). The $\Delta\chi_M T$ versus T plots also suggest that, for most of the $Cu^{II}Ln^{III}$ complexes, the exchange interactions are fairly strong, which probably could be related to the small dihedral angle (ca. 4°) between the CuO_2 and LnO_2 planes.

Introduction

Magnetic exchange interactions in 3d bimetallic complexes can now be well predicted from the molecular structures considering the symmetry and energetics of the metal orbitals containing unpaired electrons.[1] In contrast, although the lanthanide-containing exchange-coupled systems may be appealing as the building blocks for molecule-based magnets due to the large anisotropy associated with most of the lanthanides, the exchange couplings between 3d and 4f metal ions have not been much explored.[1a,2−12] In the reported 3d−4f compounds, where the nature or magnitude of the interactions has been determined, the majority of them contain gadolinium(III) as the lanthanide counterpart. The studies of the magnetic properties of exchange-coupled MGd^{III} systems (M = Cu^{II}, Ni^{II}, Co^{II}, Fe^{III}, and $V^{IV}O$) reveal that, although the nature of interaction is ferromagnetic in most cases,[2−7,11,12] the ferromagnetic behavior is not intrinsic; it depends on the environment of the metal ions and the structural parameters, and they may even turn out to be antiferromagnetic.[9c,11h,i] Further, from reported studies on $Cu^{II}Gd^{III}$ systems, it may be surmised that the extent of ferromagnetic interactions increases with a decrease of the dihedral angle between the bridging moieties of the two metal ions.[4,5,11d]

In contrast to those of $3d^nGd^{III}$ systems, the magnetic properties of heterometallic complexes of other lanthanides

* Authors to whom correspondence to be addressed. E-mail: sm_cu_chem@yahoo.co.in (S.M.); tkwei@mail.tku.edu.tw. (H.-H.W.) Fax: 91-33-23519755 (S.M.); 886-2-26209924 (H.-H.W.).
† University of Calcutta.
‡ Tamkang University.

10.1021/ic048196h CCC: $30.25
Published on Web 04/19/2005

have been sparsely investigated, and therefore, little information is available for them. It was predicted theoretically that coupling of $4f^n$ ions with other paramagnetic species will be ferromagnetic for $n > 7$ and antiferromagnetic for $n < 7$.[5] However, the reported studies do not fully corroborate this prediction.[9] The lanthanides other than Gd^{III} have a first-order orbital momentum which makes the understanding of the 3d−4f interaction complicated. Each of the $^{2S+1}L_J$ states arising from the $4f^n$ configuration due to the interelectronic repulsion and spin−orbit coupling will be further split to Stark components ($2J + 1$ if n is even, $J + 1/2$ if n is odd) due to the crystal-field perturbation. Except for Sm^{III} and Eu^{III}, the $^{2S+1}L_J$ ground state is well separated from the first excited state. At room temperature, all the Stark levels of the ground state (for Ln^{III} other than Sm^{III} and Eu^{III}) or the ground and first excited states (in the case of Sm^{III} and Eu^{III}) are populated. A progressive depopulation of these Stark sublevels takes place with a decrease of temperature. Thus, the thermal variation of the magnetic susceptibilities of the 3d−4f systems, containing anisotropic lanthanide ions, is due to both the thermal depopulations of the Stark levels and the exchange couplings. The approach that has been proposed to overcome this difficulty to understand the nature of coupling is to compare the magnetic properties of exchange-coupled 3d−4f systems with those of the structurally related species where the lanthanide ion is present in a diamagnetic environment so that the contribution due to depopulation of Stark levels can be ruled out.[9,13]

Chart 1. Chemical Structures of H_2L^1 and H_2L^2

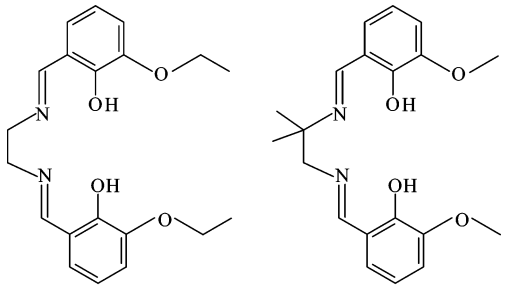

H_2L^1 H_2L^2

Compartmental Schiff base ligands derived from condensation of 3-methoxysalicylaldehyde with diaminoalkanes having alkyl substituents on the lateral alkane chain have been used to synthesize a number of discrete 3d−4f compounds.[9b,11] Using 3-ethoxysalicylaldehyde as the aldehyde functionality for compartmental Schiff base ligands suitable to stabilize the 3d−4f systems, we reported a $Cu^{II}Gd^{III}$ compound, $[Cu^{II}L^1Ln^{III}(NO_3)_3]$ (H_2L^1 = *N*,*N*′-ethylenebis(3-ethoxysalicylaldiimine, Chart 1).[4b] This complex exhibits intradimer ferromagnetic interaction ($J = 4.04$ cm^{-1}, $\mathbf{H} = -2J\mathbf{S}_1\cdot\mathbf{S}_2$). In the meantime, a few more compounds, mostly containing Gd^{III}, derived from 3-ethoxysalicylaldehyde-diamine type ligands have been reported,[4a,12] one of which exhibits the strongest ferromagnetic coupling ($J = 6.3$ cm^{-1}) among the related $Cu^{II}Gd^{III}$ compounds.[4a]

Using the ligand H_2L^2 (Chart 1), which is very similar to H_2L^1, Costes et al. reported the magnetic behavior of the $Cu^{II}Ln^{III}$ and $Ni^{II}Ln^{III}$ complexes of all the paramagnetic lanthanide(III) metals.[9b] As the nickel(II) centers in these $Ni^{II}Ln^{III}$ complexes are diamagnetic, they analyzed the nature of the interactions in the $Cu^{II}Ln^{III}$ complexes using the empirical approach. The metal centers in these compounds are either weakly coupled or noncorrelated. The dihedral angles (δ) between the CuO_2 and LnO_2 planes or NiO_2 and LnO_2 planes in these compounds are ca. 13°. Inasmuch as the value of δ in $[Cu^{II}L^1Ln^{III}(NO_3)_3]$ (4.3°) is smaller than the corresponding value (12.9°) in the $Cu^{II}Gd^{III}$ compound derived from H_2L^2, the former exhibits a stronger interaction ($J = 4.04$ cm^{-1}) than the latter ($J = 3.5$ cm^{-1}).[4b,11a] This would indicate that the $Cu^{II}Ln^{III}$ (Ln = Ce−Eu, Tb−Yb) compounds derived from H_2L^1 may exhibit stronger interactions than the feeble interactions observed in the related compounds derived from H_2L^2. In that case, similar to the $Cu^{II}Gd^{III}$

(1) (a) Kahn, O. *Molecular Magnetism*; VCH Publications: New York, 1993; see also references therein. (b) Niemann, A.; Bossek, U.; Wieghardt, K.; Butzlaff, C.; Trautwein, A. X.; Nuber, B. *Angew. Chem., Int. Ed. Engl.* **1992**, *31*, 311. (c) Merz, L.; Haase, W. *J. Chem. Soc., Dalton Trans.* **1980**, 875. (d) Thompson, L. K.; Mandal, S. K.; Tandon, S. S.; Bridson, J. N.; Park, M. K. *Inorg. Chem.* **1996**, *35*, 3117. (e) Mohanta, S.; Nanda, K. K.; Thompson, L. K.; Flörke, U.; Nag, K. *Inorg. Chem.* **1998**, *37*, 1465. (f) Chou, Y.-C.; Huang, S.-F.; Koner, R.; Lee, G.-H.; Wang, Y.; Mohanta, S.; Wei, H.-H. *Inorg. Chem.* **2004**, *43*, 2759. (g) Huang, S.-F.; Chou, Y.-C.; Misra, P.; Lee, C.-J.; Mohanta, S.; Wei, H.-H. *Inorg. Chim. Acta* **2004**, *357*, 1627.

(2) Bencini, A.; Benelli, C.; Caneschi, A.; Carlin, R. L.; Dei, A.; Gatteschi, D. *J. Am. Chem. Soc.* **1985**, *107*, 8128.

(3) (a) Winpenny, R. E. P. *Chem. Soc. Rev.* **1998**, 447. (b) Sakamoto, M.; Manseki, K.; Ōkawa, H. *Coord. Chem. Rev.* **2001**, *219*−*221*, 379.

(4) (a) Koner, R.; Lee, G.-H.; Wang, Y.; Wei, H.-H.; Mohanta, S. *Eur. J. Inorg. Chem.*, in press. (b) Mohanta, S.; Lin, H.-H.; Lee, C.-J.; Wei, H.-H. *Inorg. Chem. Commun.* **2002**, *5*, 585.

(5) Ramade, I.; Kahn, O.; Jeannin, Y.; Robert, F. *Inorg. Chem.* **1997**, *36*, 930.

(6) Sasaki, M.; Manseki, K.; Horiuchi, H.; Kumagai, M.; Sakamoto, M.; Nishida, H.; Sakiyama, Y.; Sakai, M.; Sadaoka, Y.; Ohba, M.; Ōkawa, H. *J. Chem. Soc., Dalton Trans.* **2000**, 259.

(7) Benelli, C.; Murrie, M.; Parson, S.; Winpenny, R. E. P. *J. Chem. Soc., Dalton Trans.* **1999**, 4125.

(8) (a) Westin, L. G.; Kritikos, M.; Caneschi, A. *J. Chem. Soc., Chem. Commun.* **2003**, 1012. (b) Brechin, E. K.; Harris, S. G.; Parson, S.; Winpenny, R. E. P. *J. Chem. Soc., Dalton Trans.* **1997**, 1665. (c) Sanz, J. L.; Ruiz, R.; Gleizes, A.; Lloret, F.; Faus, J.; Julve, M.; Borrás-Almenar, J.; Journaux, Y. *Inorg. Chem.* **1996**, *35*, 7384. (d) Chen, Q.-H.; Luo, Q.-H.; Wang, Z.-L.; Chen, J.-T. *J. Chem. Soc., Chem. Commun.* **2000**, 1033.

(9) (a) Kahn, M. L.; Mathonière, C.; Kahn, O. *Inorg. Chem.* **1999**, *38*, 3692. (b) Costes, J.-P.; Dupuis, A.; Laurent, J.-P. *Chem.*−*Eur. J.* **1998**, 1616. (c) Figuerola, A.; Diaz, C.; Ribas, J.; Tangoulis, V.; Granell, J.; Lloret, F.; Mahia, J.; Maestro, M. *Inorg. Chem.* **2003**, *42*, 641.

(10) Ma, B.-Q.; Gao, S.; Su, G.; Xu, G.-X. *Angew. Chem., Int. Ed.* **2001**, *40*, 434.

(11) (a) Costes, J.-P.; Dahan, F.; Dupuis, A.; Laurent, J.-P. *Inorg. Chem.* **1996**, *35*, 2400. (b) Costes, J.-P.; Dahan, F.; Dupuis, A.; Laurent, J.-P. *Inorg. Chem.* **1997**, *36*, 3429. (c) Costes, J.-P.; Dahan, F.; Dupuis, A.; Laurent, J.-P. *Inorg. Chem.* **1997**, *36*, 4284. (d) Costes, J.-P.; Dahan, F.; Dupuis, A. *Inorg. Chem.* **2000**, *39*, 165. (e) Costes, J.-P.; Dupuis, A.; Laurent, J.-P. *New J. Chem.* **1999**, 735. (f) Costes, J.-P.; Dupuis, A.; Laurent, J.-P. *Eur. J. Inorg. Chem.* **1998**, 1543. (g) Costes, J.-P.; Dupuis, A.; Laurent, J.-P. *J. Chem. Soc., Dalton Trans.* **1998**, 735. (h) Costes, J.-P.; Dahan, F.; Dupuis, A.; Laurent, J.-P. *Inorg. Chem.* **2000**, *39*, 169. (i) Costes, J.-P.; Dahan, F.; Donnadieu, B.; Garcia-Tojal, J.; Laurent, J.-P. *Eur. J. Inorg. Chem.* **2001**, 363.

(12) (a) Novitchi, G.; Shova, S.; Caneschi, A.; Costes, J.-P.; Gdaniec, M.; Stanica, N. *J. Chem. Soc., Dalton Trans.* **2004**, 1194. (b) Costes, J.-P.; Dahan, F.; Novitchi, G.; Arion, V.; Shova, S.; Lipkowski, J. *Eur. J. Inorg. Chem.* **2004**, 1530.

(13) The empirical approach was also used to determine the exchange interactions between lanthanide ions and organic radicals (Kahn, M. L.; Sutter, J.-P.; Golhen, S.; Guionneau, P.; Ouahab, L.; Kahn, O.; Chasseau, D. *J. Am. Chem. Soc.* **2000**, *122*, 3413).

systems (mentioned above), the role of δ in the extent of magnetic interactions can be verified. With a view to design strongly exchange-coupled $Cu^{II}Ln^{III}$ (Ln = Ce−Yb) compounds and to find magnetostructural correlations (at least in a qualitative sense), we report here the syntheses, structure determinations, and magnetic properties of the whole range of $Cu^{II}Ln^{III}$ and $Ni^{II}Ln^{III}$ compounds derived from H_2L^1.

Experimental Section

Materials and Physical Measurements. All the reagents and solvents were purchased from commercial sources and used as received. H_2L^1 and $[Cu^{II}L^1]\cdot H_2O$ (**1**) were prepared according to the reported methods.[4b] $[Ni^{II}L^1]\cdot H_2O$ (**2**) was prepared in the same way as **1**. Elemental (C, H, and N) analyses were performed on a Perkin-Elmer 2400 II analyzer. Variable-temperature (5−300 K) magnetic susceptibility measurements under a fixed field strength of 1 T were carried out with a Quantum Design MPMS SQUID magnetometer. Diamagnetic corrections were estimated from the Pascal constants.

Syntheses of $[M^{II}L^1Ln^{III}(NO_3)_3]$ (3−26; M = Cu or Ni; Ln = Ce−Yb). All these complexes were prepared by an experimental procedure similar to that described below for the $Cu^{II}Eu^{III}$ complex **7**, except that appropriate hydrated lanthanide(III) nitrate and the mononuclear 3d precursor $[Cu^{II}L^1]\cdot H_2O$ (**1**) or $[Ni^{II}L^1]\cdot H_2O$ (**2**) were used. Despite the variation of the metal centers, all these heterobimetallic complexes are almost identically red-colored. The elemental analyses of all the complexes are consistent with the formula $[M^{II}L^1Ln^{III}(NO_3)_3]$ (Table S1 in the Supporting Information).

A solution of $Eu(NO_3)_3\cdot 5H_2O$ (0.107 g, 0.25 mmol) in 5 mL of acetone was added to a stirred suspension of $[Cu^{II}L^1]\cdot H_2O$ (0.108 g, 0.25 mmol) in 40 mL of acetone. After a few minutes, a red solution resulted. The solution was filtered to remove the suspended materials and kept at room temperature for very slow evaporation. After a few days, red crystals suitable for X-ray diffraction were deposited which were collected by filtration, washed with acetone, and dried in a vacuum. Yield: 0.145 g (77%). Anal. Calcd for $C_{20}H_{22}N_5O_{13}CuEu$: C, 31.77; H, 2.93; N, 9.26. Found: C, 31.86; H, 3.00; N, 9.20.

Crystal Structure Determinations of 3 ($Cu^{II}Ce^{III}$), 4 ($Cu^{II}Pr^{III}$), 7 ($Cu^{II}Eu^{III}$), 9 ($Cu^{II}Tb^{III}$), 10 ($Cu^{II}Dy^{III}$), 11 ($Cu^{II}Ho^{III}$), 13 ($Cu^{II}Tm^{III}$), 14 ($Cu^{II}Yb^{III}$), 15 ($Ni^{II}Ce^{III}$), 17 ($Ni^{II}Nd^{III}$), 19 ($Ni^{II}Eu^{III}$), 21 ($Ni^{II}Tb^{III}$), and 24 ($Ni^{II}Er^{III}$). Diffraction data for all the compounds, except for **10**, were collected on a Siemens P4 diffractometer in the $\omega-2\theta$ scan mode using graphite-monochromated Mo Kα radiation having $\lambda = 0.71073$ Å. In the case of **10**, a Bruker SMART CCD diffractometer was used. Three standard reflections were periodically monitored and showed no significant variation over data collection. The accurate unit cells were obtained by means of least-squares fits of 25 centered reflections. The unit cell parameters of all these crystals are almost the same. They crystallize in the orthorhombic $P2_12_12_1$ space group, and the values of *a*, *b*, and *c* are very close. The intensity data were corrected for Lorentz and polarization effects, and semi-empirical absorption corrections were made from ψ scans. For each of the crystals, except for **10**, the total number of reflections were independent ($R_{int} = 0.0000$) and used for structure determinations. In the case of **10**, a total of 22294 reflections were collected, 5739 ($R_{int} = 0.0365$) independent reflections of which were used for structure determination. The structures were solved by direct and Fourier methods and refined by full-matrix least-squares methods based on F^2 with the programs SHELXS-97 and SHELXL-97.[14] Neutral atom scattering factors were taken from a standard source.[15] All non-hydrogen atoms were readily located and refined by

Table 1. Crystallographic Data for **3**, **4**, **7**, **9**, **10**, **11**, **13**, and **14**

	3 ($Cu^{II}Ce^{III}$)	**4** ($Cu^{II}Pr^{III}$)	**7** ($Cu^{II}Eu^{III}$)	**9** ($Cu^{II}Tb^{III}$)	**10** ($Cu^{II}Dy^{III}$)	**11** ($Cu^{II}Ho^{III}$)	**13** ($Cu^{II}Tm^{III}$)	**14** ($Cu^{II}Yb^{III}$)
empirical formula	$C_{20}H_{22}N_5O_{13}CuCe$	$C_{20}H_{22}N_5O_{13}CuPr$	$C_{20}H_{22}N_5O_{13}CuEu$	$C_{20}H_{22}N_5O_{13}CuTb$	$C_{20}H_{22}N_5O_{13}CuDy$	$C_{20}H_{22}N_5O_{13}CuHo$	$C_{20}H_{22}N_5O_{13}CuTm$	$C_{20}H_{22}N_5O_{13}CuYb$
fw	744.09	744.88	755.93	762.89	766.47	768.90	772.90	777.01
space group	$P2_12_12_1$	$P2_12_12_1$	$P2_12_12_1$	$P2_12_12_1$	$P2_12_12_1$	$P2_12_12_1$	$P2_12_12_1$	$P2_12_12_1$
a, Å	8.697(6)	8.619(5)	8.601(3)	8.611(3)	8.5870(3)	8.583(3)	8.566(3)	8.576(3)
b, Å	13.905(6)	13.8698(10)	13.786(2)	13.814(5)	13.7580(5)	13.749(3)	13.735(3)	13.705(3)
c, Å	21.176(8)	21.1269(15)	12.1483(16)	21.244(6)	21.1665(7)	21.191(3)	21.1786(19)	21.114(3)
V, Å^3	2561(2)	2525.7(15)	2507.7(9)	2527.1(14)	2500.61(15)	2500.8(10)	2491.8(10)	2481.6(12)
Z	4	4	4	4	4	4	4	4
T, K	293(2)	293(2)	293(2)	293(2)	295(2)	293(2)	293(2)	293(2)
λ(Mo Kα), Å	0.71073	0.71073	0.71073	0.71073	0.71073	0.71073	0.71073	0.71073
μ, cm^{-1}	2.662	2.826	3.405	3.695	3.894	4.070	4.470	4.682
ρ_{calcd}, g cm^{-3}	1.930	1.959	2.002	2.005	2.036	2.042	2.060	2.080
R1[a] ($I > 2\sigma(I)$)	0.0347	0.0273	0.0302	0.0289	0.0205	0.0456	0.0306	0.0447
wR2[b] (all data)	0.0889	0.0837	0.0817	0.0809	0.0452	0.1152	0.0803	0.1332

[a] $R1 = [\sum||F_o| - |F_c||/\sum|F_o|]$. [b] $wR2 = [\sum w(F_o^2 - F_c^2)^2/\sum w(F_o^2)^2]^{1/2}$.

Table 2. Crystallographic Data for **15**, **17**, **19**, **21**, and **24**

	15 ($Ni^{II}Ce^{III}$)	**17** ($Ni^{II}Nd^{III}$)	**19** ($Ni^{II}Eu^{III}$)	**21** ($Ni^{II}Tb^{III}$)	**24** ($Ni^{II}Er^{III}$)
empirical formula	$C_{20}H_{22}N_5O_{13}NiCe$	$C_{20}H_{22}N_5O_{13}NiNd$	$C_{20}H_{22}N_5O_{13}NiEu$	$C_{20}H_{22}N_5O_{13}NiTb$	$C_{20}H_{22}N_5O_{13}NiEr$
fw	739.26	743.38	751.10	758.06	766.40
space group	$P2_12_12_1$	$P2_12_12_1$	$P2_12_12_1$	$P2_12_12_1$	$P2_12_12_1$
a, Å	8.6323(12)	8.6215(15)	8.617(4)	8.607(3)	8.601(4)
b, Å	13.822(2)	13.776(4)	13.754(3)	13.742(3)	13.710(4)
c, Å	21.176(3)	21.179(3)	21.215(3)	21.240(4)	21.252(5)
V, Å^3	2526.7(6)	2515.4(9)	2514.5(12)	2512.1(11)	2506.0(14)
Z	4	4	4	4	4
T, K	293(2)	293(2)	293(2)	293(2)	293(2)
λ(Mo Kα), Å	0.71073	0.71073	0.71073	0.71073	0.71073
μ, cm^{-1}	2.602	2.868	3.298	3.620	4.156
$\rho_{calcd.}$, g cm^{-3}	1.943	1.963	1.984	2.004	2.031
R1[a] ($I > 2\sigma(I)$)	0.0250	0.0290	0.0277	0.0265	0.0253
wR2[b] (all data)	0.0707	0.0762	0.0796	0.0698	0.0705

[a] $R1 = [\sum||F_o| - |F_c||/\sum|F_o|]$. [b] $wR2 = [\sum w(F_o^2 - F_c^2)^2/\sum w(F_o^2)^2]^{1/2}$.

anisotropic thermal parameters. The final least-squares refinements (R1) based on $I > 2\sigma(I)$ converged to satisfactory values (Tables 1 and 2).

Results and Discussion

Description of the Structures of 3 ($Cu^{II}Ce^{III}$), 4 ($Cu^{II}Pr^{III}$), 7 ($Cu^{II}Eu^{III}$), 9 ($Cu^{II}Tb^{III}$), 10 ($Cu^{II}Dy^{III}$), 11 ($Cu^{II}Ho^{III}$), 13 ($Cu^{II}Tm^{III}$), 14 ($Cu^{II}Yb^{III}$), 15 ($Ni^{II}Ce^{III}$), 17 ($Ni^{II}Nd^{III}$), 19 ($Ni^{II}Eu^{III}$), 21 ($Ni^{II}Tb^{III}$), and 24 ($Ni^{II}Er^{III}$). An ORTEP representation of $[Cu^{II}L^1Eu^{III}(NO_3)_3]$, **7**, along with atom labels is shown in Figure 1, while the selected bond lengths and angles of this compound are listed in Table 3. The structure of **7** shows that it is a dinuclear neutral complex of copper(II) and europium(III). The metal centers are doubly bridged by two phenolate oxygens of the ligand. The inner salen-type cavity is occupied by copper(II), while europium(III) is present in the open and larger position of the dinucleating compartmental ligand $[L^1]^{2-}$. The bond distances of copper(II) and europium(III) with bridging phenolates are significantly different (Cu−O(1) = 1.908(5) Å, Cu−O(2) = 1.891(6) Å, Eu−O(1) = 2.350(5) Å, Eu−O(2) = 2.409(5) Å). Such differences in bond distances are expected due to their differences in ionic size and are observed in related 3d−4f compounds.[3−6,11,12] The bridge angles Cu−O(1)−Eu and Cu−O(2)−Eu are 106.1(2)° and 104.4(2)°, respectively. The dihedral angle between the best CuO(1)O(2) and EuO(1)O(2) planes is 4.0°, which suggests that the bridging moiety is almost planar; the deviations of the constituent atoms from the least-squares plane of CuO_2Eu do not exceed 0.03 Å. The europium(III) center in **7** is 10-coordinated. In addition to the phenolates, two ethoxy oxygens coordinate to this metal center. Two oxygens each from the three nitrates chelate to europium(III) to complete the coordination sphere. Three types of Eu−O distances are significantly different, and the average bond distances are Eu−O(phenolate) = 2.38 Å, Eu−O(nitrate) = 2.51 Å, and Eu−O(ethoxy) = 2.63 Å.

As mentioned above, copper(II) occupies the salen-type cavity and is coordinated to two phenolate oxygens and two imine nitrogens. The Cu−N separations, Cu−N(1) = 1.908(7) Å, Cu−N(2) = 1.907(7) Å, are in the range observed for copper(II) Schiff base compounds.[3−5] The *transoid* angles in this tetracoordinated environment do not deviate much from 180° (N(1)−Cu−O(2) = 172.6(3)°, N(2)−Cu−O(1) = 177.7(3)°), and the dihedral angles between the CuN(1)N(2) and CuO(1)O(2) planes (δ_1) and CuN(1)O(1) and CuN(2)O(2) planes (δ_2) are 7.9° and 7.5°, respectively. Evidently, the N_2O_2 moiety affords a square plane to the copper(II) ion. The donor centers are displaced alternatively up and down from the mean N_2O_2 plane by 0.079 Å (average), while the copper(II) lies just 0.041 Å below this plane. One noncoordinated nitrate oxygen (O(5B)) of the neighboring dinuclear unit occupies the apical position of copper(II) (Figure 2). The Cu−O(5B) distance is 3.168 Å, and the angles of the Cu−O(5B) axis with planar Cu−N or Cu−O bonds lie between 71.4° and 106.4°. Thus, although the coordination environment is essentially square planar, it can be considered that one nitrate of a neighboring molecule is semicoordinated to copper(II) and this metal center adopts a pseudo-square-pyramidal coordination geometry. Due to the weakly bound nitrates between neighboring molecules, the discrete di-

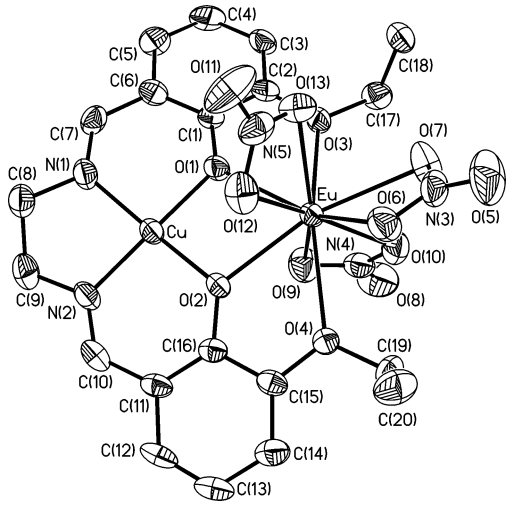

Figure 1. ORTEP representation (50% thermal ellipsoids) of the structure of $[Cu^{II}L^1Eu^{III}(NO_3)_3]$ (**7**) with atom label schemes.

(14) (a) Sheldrick, G. M. *SHELXS-97*: *A Program for Crystal Structure Solution*; University of Göttingen: Göttingen, Germany, 1997. (b) Sheldrick, G. M. *SHELXL-97*: *A Program for Crystal Structure Refinement*; University of Göttingen: Göttingen, Germany, 1993.
(15) Cromer, D. T.; Waber, J. T. *International Tables for X-ray Crystallography*; The Kynoch Press: Birmingham, U.K., 1974; Vol. IV.

Table 3. Selected Bond Lengths (Å) and Angles (deg) for **3**, **4**, **7**, **9**, **10**, **11**, **13**, and **14**

	3 ($Cu^{II}Ce^{III}$)	**4** ($Cu^{II}Pr^{III}$)	**7** ($Cu^{II}Eu^{III}$)	**9** ($Cu^{II}Tb^{III}$)	**10** ($Cu^{II}Dy^{III}$)	**11** ($Cu^{II}Ho^{III}$)	**13** ($Cu^{II}Tm^{III}$)	**14** ($Cu^{II}Yb^{III}$)
M−O(1)	1.918(7)	1.901(5)	1.908(5)	1.908(6)	1.902(2)	1.915(9)	1.904(6)	1.887(8)
M−O(2)	1.902(7)	1.901(5)	1.891(6)	1.909(7)	1.899(2)	1.908(10)	1.899(7)	1.897(9)
M−N(1)	1.921(9)	1.910(7)	1.908(7)	1.915(8)	1.915(3)	1.912(12)	1.916(8)	1.915(11)
M−N(2)	1.921(9)	1.908(7)	1.907(7)	1.915(8)	1.909(3)	1.894(13)	1.909(9)	1.893(10)
M···O(apical)	3.161	3.166	3.168	3.156	3.15	3.152	3.135	3.113
Ln−O(1)	2.437(7)	2.409(5)	2.350(5)	2.334(6)	2.318(2)	2.283(9)	2.270(7)	2.282(8)
Ln−O(2)	2.478(7)	2.445(5)	2.409(5)	2.381(6)	2.375(2)	2.371(9)	2.339(6)	2.323(9)
Ln−O(3)	2.657(7)	2.634(5)	2.600(5)	2.598(6)	2.576(2)	2.563(9)	2.554(6)	2.556(8)
Ln−O(4)	2.700(7)	2.681(5)	2.655(5)	2.657(6)	2.649(2)	2.644(9)	2.646(6)	2.637(8)
Ln−O(nitrates)	2.549(7)−2.632(8)	2.518(6)−2.603(6)	2.456(6)−2.570(6)	2.446(6)−2.565(7)	2.422(2)−2.566(2)	2.410(11)−2.588(12)	2.377(7)−2.598(9)	2.348(10)−2.622(13)
M−O(1)−Ln	106.1(3)	106.1(2)	106.1(2)	106.2(3)	106.12(9)	106.6(4)	106.3(3)	106.0(4)
M−O(2)−Ln	105.1(3)	104.8(2)	104.4(2)	104.4(3)	104.10(9)	103.5(4)	103.8(3)	104.1(3)
M···Ln[a]	3.494	3.459	3.412	3.402	3.383	3.372	3.347	3.338
M···M[b]	7.604	7.579	7.531	7.544	7.513	7.511	7.505	7.490
Ln···Ln[b]	8.697	8.619	8.601	8.611	8.587	8.583	8.566	8.576
M···Ln[b]	6.198	6.150	6.141	6.147	6.131	6.128	6.119	6.127
δ[c]	3.4	3.6	4.0	4.2	4.0	4.7	4.1	4.3
δ_1[c]	8.4	8.1	7.9	7.8	7.6	6.9	7.3	7.0
δ_2[c]	8.0	7.8	7.5	7.5	7.3	6.6	7.1	6.8
C(8A)···O(11)	3.288	3.275	3.260	3.277	3.265	3.249	3.253	3.272
H(8AA)···O(11)	2.434	2.421	2.391	2.399	2.388	2.361	2.373	2.394
C(8A)−H(8A)···O(11)	146.6	146.5	148.9	150.4	150.3	152.0	150.6	150.4
C(10C)···O(11)	3.298	3.265	3.289	3.293	3.288	3.291	3.304	3.294
H(10C)···O(11)	2.384	2.353	2.374	2.377	2.374	2.373	2.385	2.381
C(10)−H(10C)···O(11)	167.5	166.7	167.8	168.6	167.5	169.3	169.6	166.8

[a] Intramolecular. [b] Shortest intermolecular. [c] δ, δ_1, and δ_2 are, respectively, the dihedral angles between the MO(1)O(2) and LnO(1)O(2), MN(1)N(2) and MO(1)O(2), and MN(1)O(1) and MN(2)O(2) planes. Symmetry: A, $1 + x, y, z$; C, $1 - x, 0.5 + y, 0.5 - z$.

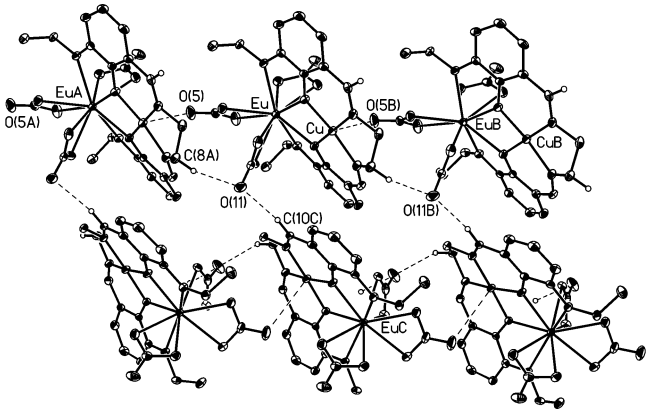

Figure 2. Perspective view to illsutrate the two-dimensional structure of $[Cu^{II}L^{1}Eu^{III}(NO_3)_3]$ (**7**). Except two hydrogens participating in hydrogen bonds, the hydrogens are omitted for clarity. Symmetry: A, $1 + x, y, z$; B, $x - 1, y, z$; C, $1 - x, 0.5 + y, 0.5 - z$.

nuclear units form one-dimensional zigzag chains running parallel to the crystallographic *a* axis.

There is no intramolecular hydrogen bonding in this molecule. However, the nitrate oxygens interact weakly with the hydrogens of the imine moieties and alkyl side chains of the neighboring molecules. Among three noncoordinated nitrate oxygens within a molecule, O(5) is weakly bound to the copper(II) center (CuA) of the neighboring unit, O(11) forms two hydrogen bonds, and the third noncoordinated oxygen (O(8)) is devoid of any electronic interaction. Among two H-bonds involving O(11), the first one takes place with the H(8AA) bonded to C(8A) of the lateral diiminoalkyl side chain of the same neighboring molecule of the one-dimensional chain to which O(5) is weakly coordinated with copper(II), while the second H-bond is formed with the imine hydrogen (H(10C)) of another adjacent molecule of a different chain (H-bond geometries (distances in angstroms, angles in degrees): H(8AA)···O(11) = 2.391, C(8A)···O(11) = 3.260, C(8A)−H(8AA)···O(11) = 148.9; H(10C)···O(11) = 2.374, C(10C)···O(11) = 3.289, C(10C)−H(10C)···O(11) = 167.8). As the H···O distances are within the sum of the van der Waals radii of H and N (2.70 Å) and the C−H···O angles do not deviate much from linearity, there is no doubt of identifying C−H···O hydrogen bonds in **7** or in other complexes reported here (vide infra).[16] Evidently, the intermolecular semicoordination of nitrate to copper(II) and H(8A)···O(11) types of intermolecular hydrogen bonds result in the formation of a one-dimensional zigzag chain of the dinuclear units, and the one-dimensional chains are stitched to two-dimensional sheets (in the *ab* plane) by the O(11)···H(10C) types of intermolecular H-bonds.

Despite the strong H-bonds as well as semicoordination of the nitrate group to the copper(II) of a neighboring molecule, the dinuclear units are so oriented in the crystal packing that the closest separations between the paramagnetic centers of adjacent molecules are rather large. The shortest intermolecular Eu···Eu and Cu···Eu distances, 8.601 and 6.141 Å, respectively, are the separations of the metal ions between adjacent molecules in the zigzag chain, while the closest Cu···Cu approach of 7.531 Å is the distance of the copper(II) centers between the neighboring molecules of two different chains.

The dinuclear cores, the semicoordination by the O(5) oxygen of the nitrates to the copper(II) or nickel(II) of a neighboring molecule, and the patterns of the intermolecular H-bonds of the $Cu^{II}Ce^{III}$ (**3**), $Cu^{II}Pr^{III}$ (**4**), $Cu^{II}Tb^{III}$ (**9**), $Cu^{II}Dy^{III}$ (**10**), $Cu^{II}Ho^{III}$ (**11**), $Cu^{II}Tm^{III}$ (**13**), $Cu^{II}Yb^{III}$ (1**4**), $Ni^{II}Ce^{III}$ (**15**), $Ni^{II}Nd^{III}$ (**17**), and $Ni^{II}Eu^{III}$ (**19**) complexes are of types similar to those described above for **7**. Thus, all the heterodinuclear compounds reported in this paper are isostructural. It may be noted that the structure of the $Cu^{II}Gd^{III}$

Table 4. Selected Bond Lengths (Å) and Angles (deg) for **15**, **17**, **19**, **21**, and **24**

	15 ($Ni^{II}Ce^{III}$)	**17** ($Ni^{II}Nd^{III}$)	**19** ($Ni^{II}Eu^{III}$)	**21** ($Ni^{II}Tb^{III}$)	**24** ($Ni^{II}Er^{III}$)
M−O(1)	1.858(4)	1.866(5)	1.865(5)	1.864(4)	1.857(5)
M−O(2)	1.866(4)	1.861(5)	1.858(5)	1.855(4)	1.850(5)
M−N(1)	1.841(5)	1.850(6)	1.842(6)	1.834(6)	1.837(7)
M−N(2)	1.848(5)	1.832(6)	1.844(6)	1.840(5)	1.846(6)
M···O(apical)	3.414	3.424	3.405	3.398	3.382
Ln−O(1)	2.439(4)	2.407(5)	2.371(4)	2.341(4)	2.313(5)
Ln−O(2)	2.477(4)	2.447(5)	2.419(5)	2.402(4)	2.375(5)
Ln−O(3)	2.615(4)	2.591(5)	2.580(5)	2.558(4)	2.536(5)
Ln−O(4)	2.641(4)	2.626(5)	2.606(5)	2.608(4)	2.599(5)
Ln−O(nitrates)	2.534(5)−2.600(5)	2.502(6)−2.573(6)	2.465(5)−2.555(6)	2.443(5)−2.553(5)	2.402(6)−2.553(6)
M−O(1)−Ln	107.83(17)	107.5(2)	107.8(2)	107.96(19)	108.0(2)
M−O(2)−Ln	106.09(15)	106.1(2)	106.11(18)	105.87(17)	105.7(2)
M···Ln[a]	3.490	3.461	3.434	3.413	3.384
M···M[b]	7.540	7.511	7.494	7.483	7.465
Ln···Ln[b]	8.632	8.622	8.617	8.607	8.601
M···Ln[b]	6.207	6.205	6.202	6.196	6.194
δ[c]	6.1	6.2	6.2	6.7	6.5
δ_1[c]	6.7	6.4	5.8	5.9	5.6
δ_2[c]	6.2	5.9	5.4	5.3	5.1
C(8A)···O(11)	3.282	3.268	3.285	3.297	3.280
H(8AA)···O(11)	2.430	2.409	2.419	2.425	2.402
C(8A)−H(8A)···O(11)	146.5	147.4	148.4	149.5	150.3
C(10C)···O(11)	3.298	3.312	3.316	3.310	3.329
H(10C)···O(11)	2.379	2.394	2.399	2.397	2.404
C(10)···H(10C)···O(11)	169.6	169.4	169.0	167.0	172.6

[a] Intramolecular. [b] Shortest intermolecular. [c] δ, δ_1, and δ_2 are, respectively, the dihedral angles between the MO(1)O(2) and LnO(1)O(2), MN(1)N(2) and MO(1)O(2), and MN(1)O(1) and MN(2)O(2) planes. Symmetry: A, $1 + x, y, z$; C, $1 - x, 0.5 + y, 0.5 - z$.

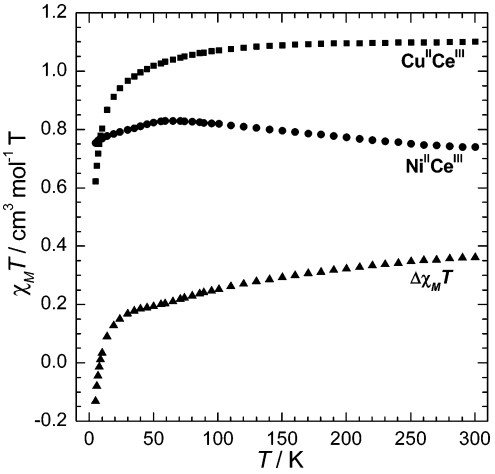

Figure 3. Temperature dependence of $\chi_M T$ for **3** ($Cu^{II}Ce^{III}$) and **15** ($Ni^{II}Ce^{III}$) and $\Delta\chi_M T$ between the succeptibilities of these two compounds.

complex $[Cu^{II}L^1Gd^{III}(NO_3)_3]$ (**8**) is also similar to the structures described here.[4b] The ORTEP of the dinuclear core and the two-dimensional sheet structure of a nickel(II) analogue, **15**, are shown, respectively, in Figures S1 and S2 of the Supporting Information, while the selected bond lengths and angles of all the structurally characterized compounds are listed in Tables 3 and 4.

Due to lanthanide contraction, the bond lengths involving lanthanides and the intramolecular metal−metal separations in the $Cu^{II}Ln^{III}$ or $Ni^{II}Ln^{III}$ complexes decrease with an increase of the atomic number of the lanthanides. As compared to those of copper(II), the bond distances of nickel(II) are relatively shorter and the N_2O_2 donor centers afford a better square plane for nickel(II) as indicated by δ_1 and δ_2 (Tables 3 and 4). The same parameters reveal that, for the whole series, the extent of planarity of either Cu^{II} or Ni^{II} environments increases slightly but systematically on going from lower to higher members of the lanthanide series. Although the dihedral angles (δ) between the MO(1)O(2) and LnO(1)O(2) planes for both the $Ni^{II}Ln^{III}$ and $Cu^{II}Ln^{III}$ complexes increase from the lower to the higher analogues, the differences are too small (δ values for the $Cu^{II}Ce^{III}$, $Cu^{II}Yb^{III}$, $Ni^{II}Ce^{III}$, and $Ni^{II}Er^{III}$ complexes are 3.4°, 4.3°, 6.1°, and 6.5°, respectively). The comparison of the structural parameters in the $Cu^{II}Ce^{III}$ versus $Ni^{II}Ce^{III}$, $Cu^{II}Eu^{III}$ versus $Ni^{II}Eu^{III}$, and $Cu^{II}Tb^{III}$ versus $Ni^{II}Tb^{III}$ complexes indicates that, except for the slight differences in the Ln−OEt bond lengths, the bond distances of the lanthanides remain almost identical for a pair of compounds.

Magnetic Properties

Variable-Temperature (5−300 K) Magnetic Behavior of the $Ni^{II}Ln^{III}$ Complexes 15−26. The $\chi_M T$ versus T plots of the $Ni^{II}Ln^{III}$ complexes are shown in Figures 3−9 and S3−S7 in the Supporting Information. For the $Ni^{II}Gd^{III}$ complex (**20**), $\chi_M T$ values in the 300−5 K temperature range are almost constant and equal to the calculated value (7.88 $cm^3\ mol^{-1}\ K$) expected for only gadolinium(III) having an $^8S_{7/2}$ ground state, indicating the diamagnetic nature of the Ni^{II} center. Evidently, the susceptibilities of all the $Ni^{II}Ln^{III}$ complexes reported here arise only due to the lanthanide(III) ions.

The room temperature $\chi_M T$ values (0.74, 1.40, 1.45, 0.28, and 1.39 $cm^3\ mol^{-1}\ K$, respectively, for **15** ($Ni^{II}Ce^{III}$), **16**

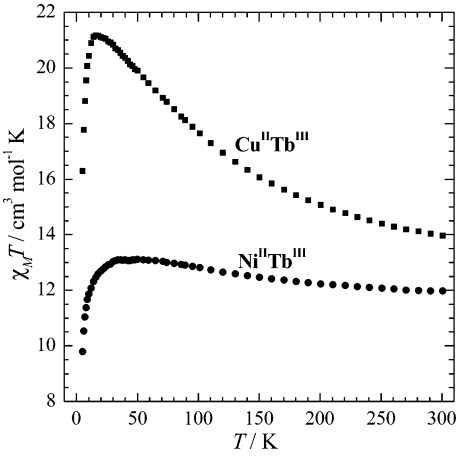

Figure 4. Temperature dependence of $\chi_M T$ for **9** ($Cu^{II}Tb^{III}$) and **21** ($Ni^{II}Tb^{III}$).

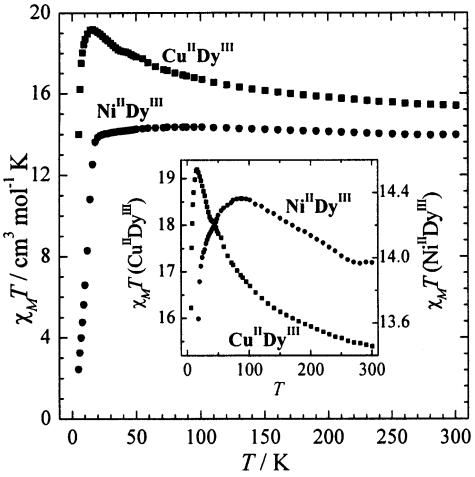

Figure 5. Temperature dependence of $\chi_M T$ for **10** ($Cu^{II}Dy^{III}$) and **22** ($Ni^{II}Dy^{III}$). Inset: on expanding the $\chi_M T$ axis, parts of the plots have been shown for the clear demonstration of the maxima as well as the steep increase of $\chi_M T$.

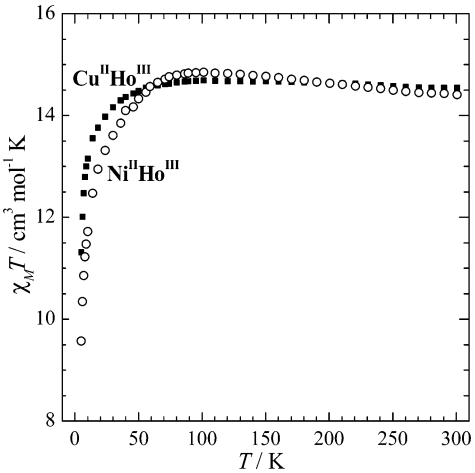

Figure 6. Temperature dependence of $\chi_M T$ for **11** ($Cu^{II}Ho^{III}$) and **23** ($Ni^{II}Ho^{III}$).

(16) (a) Desiraju, G. R. *Acc. Chem. Res.* **2002**, *35*, 565. (b) Senthil Kumar, V. S.; Christopher, F.; Rath, N. P. *Cryst. Growth Des.* **2004**, *4*, 651.

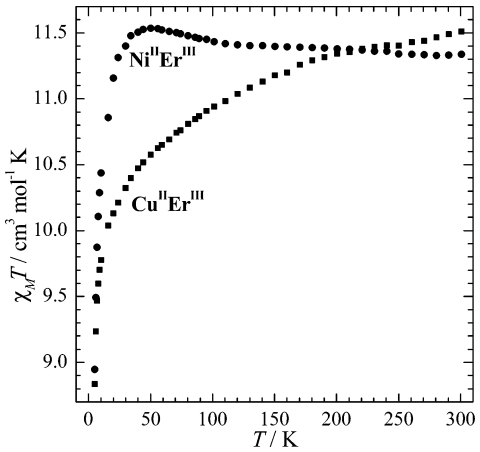

Figure 7. Temperature dependence of $\chi_M T$ for **12** ($Cu^{II}Er^{III}$) and **24** ($Ni^{II}Er^{III}$).

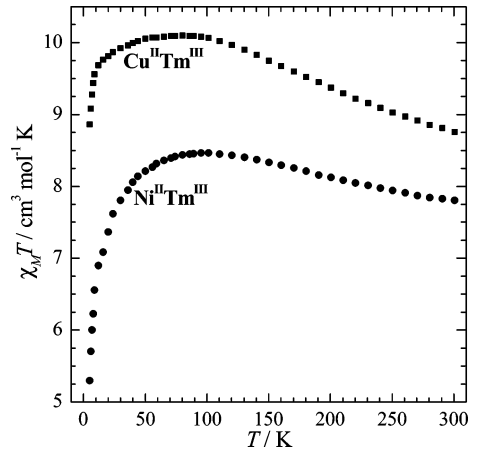

Figure 8. Temperature dependence of $\chi_M T$ for **13** ($Cu^{II}Tm^{III}$) and **25** ($Ni^{II}Tm^{III}$).

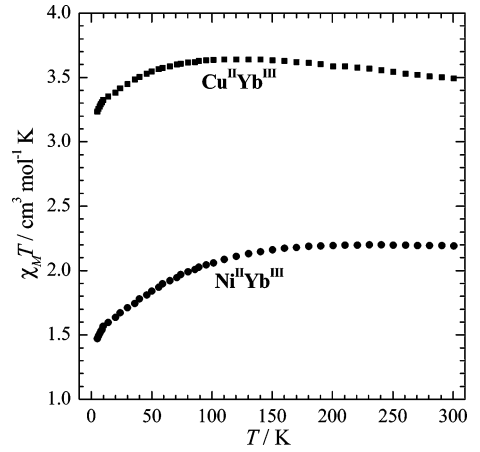

Figure 9. Temperature dependence of $\chi_M T$ for **14** ($Cu^{II}Yb^{III}$) and **26** ($Ni^{II}Yb^{III}$).

($Ni^{II}Pr^{III}$), **17** ($Ni^{II}Nd^{III}$), **18** ($Ni^{II}Sm^{III}$), and **19** ($Ni^{II}Eu^{III}$)) of the $Ni^{II}Ln^{III}$ compounds are slightly lower than the theoretical values (0.80, 1.60, 1.64, 0.32, and 1.63 $cm^3\ mol^{-1}$ K, respectively, for **15**, **16**, **17**, **18**, and **19**) of the free ions considering the ground states (for Ce^{III}, Pr^{III}, and Nd^{III}) or ground and first excited states (for Sm^{III} and Eu^{III}) of the lanthanides. Except for **15** ($Ni^{II}Ce^{III}$), the magnetic behavior of these $Ni^{II}Ln^{III}$ complexes are characterized by a continuous decrease of $\chi_M T$ on lowering of the temperature. The $\chi_M T$ values at 5 K of **19** ($Ni^{II}Eu^{III}$) and **16** ($Ni^{II}Pr^{III}$) (0.037 and 0.12 $cm^3\ mol^{-1}$ K, respectively) as well as the trends at low temperatures indicate that the low-temperature limit of $\chi_M T$ for these two complexes is vanishingly small. As the ground state ($^4F_0$) of Eu^{III} and the lowest energy Stark component ($M_J = 0$) of the $^3H_4$ ground level of Pr^{III} are nonmagnetic, the observations made are justifiably consistent. In the case of the $Ni^{II}Sm^{III}$ complex **18**, almost linear variation of $\chi_M T$ with T and a very small $\chi_M T$ value at low temperatures (0.034 $cm^3\ mol^{-1}$ K at 5 K) are similar to those reported for the mononuclear Sm^{III} compounds.[13] For the $Ni^{II}Ce^{III}$ complex **15**, the $\chi_M T$ values slowly increase from 300 K (0.74 $cm^3\ mol^{-1}$ K) to 65 K (0.83 $cm^3\ mol^{-1}$ K) and then decrease, again slowly, up to 5 K (0.76 $cm^3\ mol^{-1}$ K).

Similar to those of complexes **15**−**19**, the $\chi_M T$ values at 300 K for the $Ni^{II}Dy^{III}$ (**22**), $Ni^{II}Er^{III}$ (**24**), and $Ni^{II}Yb^{III}$ (**26**) complexes are slightly lower (13.97, 11.33, and 2.19 $cm^3\ mol^{-1}$ K, respectively, for **22**, **24**, and **26**) than the theoretical values (14.12, 11.45, and 2.53 $cm^3\ mol^{-1}$ K, respectively, for **22**, **24**, and **26)**. In contrast, the $\chi_M T$ values at 300 K of the $Ni^{II}Ln^{III}$ complexes of the other higher analogues are a little higher than the calculated values (observed values/$cm^3\ mol^{-1}$ K [**21** ($Ni^{II}Tb^{III}$)] 11.97, [**23** ($Ni^{II}Ho^{III}$)] 14.40, [**25** ($Ni^{II}Tm^{III}$)] 7.80; calculated values/$cm^3\ mol^{-1}$ K [**21** ($Ni^{II}Tb^{III}$)] 11.81, [**23** ($Ni^{II}Ho^{III}$)] 14.04, [**25** ($Ni^{II}Tm^{III}$)] 7.28). On lowering of the temperature from 300 K, except for the $Ni^{II}Yb^{III}$ complex **26**, $\chi_M T$ of the other $Ni^{II}Ln^{III}$ complexes (**21**−**25**) increases slowly to reach a maximum and then diminishes rapidly on further cooling. The temperature ranges (K) for the maximum and the corresponding $\chi_M T$ values ($cm^3\ mol^{-1}$ K) of these complexes are [**21** ($Ni^{II}Tb^{III}$)] 60−32, 13.0, [**22** ($Ni^{II}Dy^{III}$)] 100−75, 14.35, [**23** ($Ni^{II}Ho^{III}$)] 108−86, 14.82, [**24** ($Ni^{II}Er^{III}$)] 50, 11.54, and [**25** ($Ni^{II}Tm^{III}$)] 105−80, 8.45. In the lower temperature range, a rapid decrease of the $\chi_M T$ values takes place to reach 9.78, 2.45, 9.56, 8.94, and 5.3 $cm^3\ mol^{-1}$ K at 5 K for **21**, **22**, **23**, **24**, and **25**, respectively. In contrast to the other higher analogues, the $\chi_M T$ values of the $Ni^{II}Yb^{III}$ complex **26** remain almost constant in the temperature range 300−200 K. On further cooling, $\chi_M T$ sharply decreases to 1.47 $cm^3\ mol^{-1}$ K at 5 K.

It is clear from the above discussion that the $\chi_M T$ versus T profiles of the $Ni^{II}Ln^{III}$ complexes do not obey the Curie law. On lowering of the temperature, progressive depopulation of the Stark levels, which arise in the crystal field of the anisotropic Ln^{III} ions, takes place. Due to these types of population variation, as observed in **16**−**19** ($Ni^{II}Pr^{III}$−$Ni^{II}Eu^{III}$) and **26** ($Ni^{II}Yb^{III}$), the $\chi_M T$ values should be expected to diminish gradually on steady cooling of the compounds. Evidently, the initial increase of $\chi_M T$ to reach a maximum for the $Ni^{II}Ln^{III}$ (Ln = Ce (**15**), Tb−Tm (**21**−**25**)) complexes is rather peculiar and is difficult to explain at this stage. Although a mononuclear Ce^{III} compound is known to exhibit a similar type of magnetic behavior,[13] the initial increase of $\chi_M T$ on lowering of the temperature was not previously observed for the other examples, which show a gradual decrease of $\chi_M T$ on lowering of the temperature.[9,12b]

Variable-Temperature (5−300 K) Magnetic Behavior of the $Cu^{II}Ln^{III}$ Complexes 3−14. The $\chi_M T$ versus T plots

of the $Cu^{II}Ln^{III}$ complexes are shown in Figures 3−9 and S3−S7. The room temperature $\chi_M T$ values (1.10, 1.75, 1.45, 0.66, and 1.82 $cm^3\ mol^{-1}$ K, respectively for **3** ($Cu^{II}Ce^{III}$), **4** ($Cu^{II}Pr^{III}$), **5** ($Cu^{II}Nd^{III}$), **6** ($Cu^{II}Sm^{III}$), and **7** ($Cu^{II}Eu^{III}$)) of the $Cu^{II}Ln^{III}$ complexes are again slightly lower than the theoretical values (1.18, 1.78, 1.79, 0.65, and 1.84 $cm^3\ mol^{-1}$ K, respectively) expected for the noninteracting metal ions. However, taking the observed values of the $Ni^{II}Ln^{III}$ complexes as the single-ion $\chi_M T$ of the lanthanides, the experimental $\chi_M T$ values of the $Cu^{II}Ln^{III}$ compounds (Ln = Ce−Eu) match well with those expected for isolated Cu^{II} and Ln^{III} ions. As shown in Figures 3 and S4−S7, $\chi_M T$ of all these $Cu^{II}Ln^{III}$ complexes decreases on lowering of the temperature from 300 to 5 K. Except for the $Cu^{II}Eu^{III}$ complex **7**, for which the variation is gradual throughout the temperature range, the decrease of $\chi_M T$ below 50−60 K for the Ce^{III}, Pr^{III}, Nd^{III}, and Sm^{III} systems is quite sharp.

Among the $Cu^{II}Ln^{III}$ complexes of the $f^{n>7}$ lanthanides, Tb^{III} (**9**), Dy^{III} (**10**), Tm^{III} (**13**), and Yb^{III} (**14**) compounds exhibit room temperature $\chi_M T$ values (13.96, 15.40, 8.76, and 3.49 $cm^3\ mol^{-1}$ K, respectively), much higher than the theoretical values (12.18, 14.50, 7.65, and 2.90 $cm^3\ mol^{-1}$ K, respectively) expected for noninteracting metal ions. In contrast, the $\chi_M T$ values of the $Cu^{II}Ho^{III}$ (**11**, 14.54 $cm^3\ mol^{-1}$ K) and $Cu^{II}Er^{III}$ (**12**, 11.51 $cm^3\ mol^{-1}$ K) complexes deviate only slightly form the calculated values (14.42 and 11.82 $cm^3\ mol^{-1}$ K, respectively). On lowering of the temperature from 300 K, the $\chi_M T$ values of the $Cu^{II}Tb^{III}$ complex **9** increase surprisingly rapidly to reach a maximum of 20.94 $cm^3\ mol^{-1}$ K at 26 K and then decrease to 16.29 $cm^3\ mol^{-1}$ K at 5 K. Similarly, with the lowering of the temperature, the $\chi_M T$ values of the $Cu^{II}Dy^{III}$ complex **10** increase to reach a maximum at 16 K (19.19 $cm^3\ mol^{-1}$ K) and then sharply fall to 14 $cm^3\ mol^{-1}$ K at 5 K. The profiles of the $\chi_M T$ versus T plots of the Tm^{III} (**13**) and Yb^{III} (**14**) compounds are of similar types. In these two systems, the $\chi_M T$ values increase initially to a maximum (10.08 and 3.64 $cm^3\ mol^{-1}$ K, respectively) in a particular temperature range (95−60 and 140−100 K, respectively) and then sharply decrease on further lowering of the temperature ($\chi_M T$ values at 5 K: 8.86 $cm^3\ mol^{-1}$ K for **13** ($Cu^{II}Tm^{III}$) and 3.23 $cm^3\ mol^{-1}$ K for **14** ($Cu^{II}Yb^{III}$)). In sharp contrast to those of the other higher analogues, the profile of the $Cu^{II}Er^{III}$ complex **12** is characterized by a continuous decrease of the $\chi_M T$ values; $\chi_M T$ decreases slowly from 11.51 to 10.39 $cm^3\ mol^{-1}$ K in the temperature range 300−35 K and then decreases rapidly to 8.83 $cm^3\ mol^{-1}$ K at 5 K.

Analysis of the Nature of the Magnetic Exchange Interactions Using the $\Delta\chi_M T$ versus T Plots. As mentioned earlier and described for the $Ni^{II}Ln^{III}$ systems, the intrinsic $\chi_M T$ of the lanthanides, other than gadolinium(III), varies with temperature. Thus, the temperature dependence of the magnetic susceptibilities of the $Cu^{II}Ln^{III}$ compounds is a superposition of the variation of the intrinsic susceptibilities of Ln^{III} and exchange interaction, if there exists any, between Cu^{II} and Ln^{III} centers. We have used an empirical approach[9a] to understand the nature of the magnetic exchange interactions between copper(II) and lanthanide(III) in these $Cu^{II}Ln^{III}$ complexes **3**−**14**. The structures of the $Ni^{II}Ln^{III}$ and $Cu^{II}Ln^{III}$ complexes are similar. The Cu^{II} and Ni^{II} complexes with a particular lanthanide preserve the same space group of the unit cell, unit cell contents, and most of the structural parameters around the lanthanide ion. Only marginal differences are observed in the Ln−OEt distances. It is logical therefore to assume that, for a given Ln^{III} ion, the crystal field around it will be the same for $Cu^{II}Ln^{III}$ and $Ni^{II}Ln^{III}$ analogues. Thus, the temperature dependence of the intrinsic magnetic susceptibilities of any lanthanide can be expected to be identical in both the systems. The structural data suggest that the dinuclear cores are well separated. Only weak intermolecular interactions are possible through the weakly bound nitrates and H-bonding networks. Even for the ferromagnetically coupled $Cu^{II}Gd^{III}$ compound **8** having the ground-state $S_T = 4$ at low temperatures, the intermolecular exchange interaction has been found to be extremely weak ($J' = -0.006\ cm^{-1}$).[4b] Thus, the possibility of intermolecular interactions in the other $Cu^{II}Ln^{III}$ complexes can be considered to be negligible. Therefore, the difference in $\chi_M T$ between a $Cu^{II}Ln^{III}$ complex and the corresponding $Ni^{II}Ln^{III}$ analogue ($\Delta\chi_M T$) and its variation with temperature can be regarded to arise only due to the magnetic exchange interactions between Cu^{II} and Ln^{III}. The interaction will be antiferromagnetic if the profile of $\Delta\chi_M T$ versus T exhibits a descending pattern on lowering of the temperature and ferromagnetic with the reversal of trends. On the other hand, if $\Delta\chi_M T$ remains independent of T throughout the temperature range, then the two metal ions can be regarded as magnetically noninteractiong. It should be mentioned that this empirical approach has been used previously to gain ideas of the exchange interactions in discrete[9b] and 2-D[9a] $Cu^{II}Ln^{III}$, dinuclear cyano-bridged $Fe^{III}Ln^{III}$,[9c] and Ln^{III}-radical systems.[13]

The $\Delta\chi_M T$ versus T plots for the lower analogues (Ce^{III}−Eu^{III}) are shown in Figures 3 and S4−S7. The values of $\Delta\chi_M T$ at 300 K are in the range 0.35−0.42 $cm^3\ mol^{-1}$ K, very close to the spin-only $\chi_M T$ value of 0.38 $cm^3\ mol^{-1}$ K for the Cu^{II} ion. For the Ce^{III} and Nd^{III} compounds, $\Delta\chi_M T$ decreases slowly from 300 K to around 50 K (value at 50 K: 0.2 $cm^3\ mol^{-1}$ K for Ce^{III} and 0.18 $cm^3\ mol^{-1}$ K for Nd^{III}), while it remains almost constant in this temperature range for the Sm^{III} system. However, below 50 K, the $\Delta\chi_M T$ values sharply decrease for all three cases. The profiles clearly indicate that antiferromagnetic couplings are operating in the $Cu^{II}Ce^{III}$ (**3**), $Cu^{II}Nd^{III}$ (**5**), and $Cu^{II}Sm^{III}$ (**6**) complexes. The sharp decrease of $\Delta\chi_M T$ below 50 K may be due to the feeble nature of the exchange coupling, so this is more perceptible at low temperatures. For the Ce^{III}, Nd^{III}, and Sm^{III} complexes the differences in $\Delta\chi_M T$ between 300 and 5 K are 0.49, 0.92, and 0.23 $cm^3\ mol^{-1}$ K, respectively. In contrast, the $\Delta\chi_M T$ values of the Pr^{III} and Eu^{III} complexes show only a small change (0.08 and 0.04 $cm^3\ mol^{-1}$ K, respectively) for the entire temperature range, indicating that the metal centers in these two complexes are noncorrelated.

As illustrated by the $\Delta\chi_M T$ versus T plots in Figures 10−12, all of the $Cu^{II}Ln^{III}$ complexes with an $f^{n>7}$ lanthanide(III) exhibit unusual magnetic behavior. $\Delta\chi_M T$ of the Tb^{III}

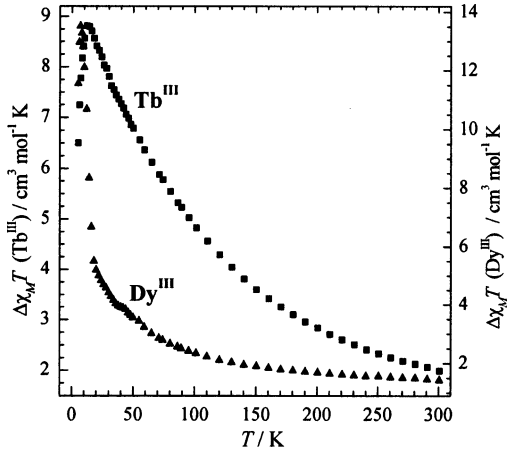

Figure 10. Temperature dependence of $\Delta\chi_M T$ for the Tb^{III} and Dy^{III} compounds.

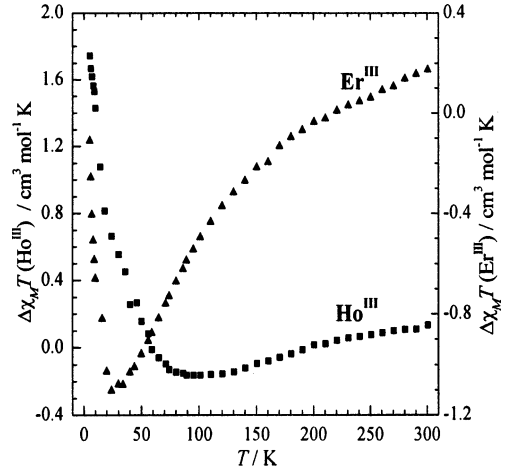

Figure 11. Temperature dependence of $\Delta\chi_M T$ for the Ho^{III} and Er^{III} compounds.

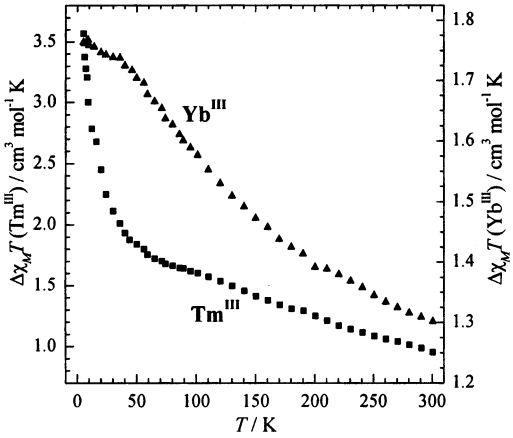

Figure 12. Temperature dependence of $\Delta\chi_M T$ for the Tm^{III} and Yb^{III} compounds.

case increases very rapidly from 1.99 to 8.71 $cm^3\ mol^{-1}$ K in the temperature range 300−16 K and then decreases sharply to 6.50 $cm^3\ mol^{-1}$ K at 5 K. In the case of the Dy^{III} complex, $\Delta\chi_M T$ increases slowly from 1.43 to 2.35 $cm^3\ mol^{-1}$ K in the temperature range 300−100 K and then more rapidly to 5.20 $cm^3\ mol^{-1}$ K at 20 K. Finally, below 20 K, $\Delta\chi_M T$ increases abruptly rapidly to 13.57 $cm^3\ mol^{-1}$ K at 7 K before it falls to 11.55 $cm^3\ mol^{-1}$ K at 5 K. Clearly, the metal centers are ferromagnetically coupled in this case also. The decrease of $\Delta\chi_M T$ at very low temperatures may be due to the intermolecular interaction. It should be noted that a similar type of intermolecular interaction has also been observed in the $Cu^{II}Gd^{III}$ complex **8** derived from the same ligand.[4b] The semicoordination by the nitrates is the probable source of the intermolecular interaction. $\Delta\chi_M T$ for the Yb^{III} compound increases steadily from 1.30 to 1.76 $cm^3\ mol^{-1}$ K in the whole temperature range, while, in the case of the Tm^{III} complex, it increases slowly from 0.95 $cm^3\ mol^{-1}$ K at 300 K to 2.01 $cm^3\ mol^{-1}$ K at 36 K and then rapidly increases to 3.56 $cm^3\ mol^{-1}$ K at 5 K. The $\Delta\chi_M T$ versus T profiles indicate the existence of ferromagnetic interactions in these two cases also. In contrast, the $\Delta\chi_M T$ values of the Ho^{III} (0.14 $cm^3\ mol^{-1}$ K) and Er^{III} (0.17 $cm^3\ mol^{-1}$ K) complexes at 300 K are small, smaller than the value expected for copper(II) alone. $\Delta\chi_M T$ of these two cases passes through a minimum (−0.014 $cm^3\ mol^{-1}$ K at 120−80 K for Ho^{III} and −1.08 $cm^3\ mol^{-1}$ K at 35−20 K for Er^{III}) and then increases very rapidly ($\Delta\chi_M T$ values at 5 K: 1.74 $cm^3\ mol^{-1}$ K for Ho^{III} and −0.11 $cm^3\ mol^{-1}$ K for Er^{III}). The intermolecular interactions in the Gd^{III}, Tb^{III}, and Dy^{III} compounds are antiferromagnetic. If the intermolecular interactions in the Ho^{III} and Er^{III} compounds are ferromagnetic, then the $\Delta\chi_M T$ values may increase at lower temperatures. Although this explaination may be considered as logical for the Er^{III} compound for which the minimum appears at 35−20 K; however, the intermolecular interaction around 80 K (for the Ho^{III} compound) will not be a good proposition. Moreover, below the minimum, $\Delta\chi_M T$ increases rapidly to a significantly higher value (1.73 $cm^3\ mol^{-1}$ K in comparison to 0.38 $cm^3\ mol^{-1}$ K for the Cu^{II} ion). This clearly indicates that the interaction in the Ho^{III} compound is also ferromagnetic; the coupling is perceptible at relatively lower temperatures than those of the Tb^{III}, Dy^{III}, Tm^{III}, and Yb^{III} compounds. However, for the Ho^{III} compound, it is difficult to comment on the reasons for the initial lowering of $\Delta\chi_M T$ or the smaller value of the $\Delta\chi_M T$ in the higher temperature range. For the Er^{III} compound, except in the 300−200 K temperature range, $\Delta\chi_M T$ is negative; even below the minimum, $\Delta\chi_M T$ increases to only −0.11 $cm^3\ mol^{-1}$ K at 5 K. Therefore, at present, no conclusion should be drawn regarding the nature of the interaction in the Er^{III} compound.

Comparison of the Nature of the Magnetic Interactions in 3−14 with Those of Reported Cases. For $4f^1$−$4f^6$ configurations, Kahn et al.[5,9a] proposed that the orbital and spin momenta of Ln^{III} are antiparallel and the ferromagnetic spin coupling will give rise to an overall antiferromagnetic interaction between the angular momenta. In contrast, the orbital and spin momenta are parallel for $4f^8$−$4f^{13}$ configurations and the ferromagnetic spin coupling will result in an overall ferromagnetic interaction. Previously, Costes et al.[9b] and Kahn et al.[9a] examined the nature of the exchange interactions between copper(II) and lanthanide(III) in diphenoxo-bridged discrete dinuclear and oxamato-bridged infinite ladder types of systems. The $Cu^{II}Eu^{III}$ case was not examined by Kahn and co-workers. For lanthanides with less than half-filled configurations, they found antiferromagnetic interac-

Table 5. Natures of the Magnetic Exchange Interactions[a] in Different Types of Systems Involving Lanthanides as One of the Spin Carriers

compound	Ce	Pr	Nd	Sm	Eu	Gd	Tb	Dy	Ho	Er	Tm	Yb
phenoxo-bridged $Cu^{II}Ln^{III}$ [b]	AF	NI	AF	AF	NI	F	F	F	F	F	AF	AF
phenoxo-bridged $Cu^{II}Ln^{III}$ [c]	AF	NI	AF	AF	NI	F	F	F	F	?	F	F
oxamato-bridged 2-D $Cu^{II}Ln^{III}$ [d]	AF	AF	AF	AF		F	F	F	AF	AF	?	AF
cyano-bridged $Fe^{III}Ln^{III}$ [e]	AF	NI	AF	NI	NI	AF	F	AF	F	NI	F	NI
radical complex, $R-Ln^{III}-R$ [f]	AF	AF	AF	AF	?	F	F	F	F			

[a] F = ferromagnetic, AF = antiferromagnetic, and NI = no interaction. [b] Reference 9b. [c] This work. [d] Reference 9a. [e] Reference 9c. [f] Reference 13.

tions. The Costes group concluded the interactions in the Ce^{III}, Nd^{III}, and Sm^{III} compounds are antiferromagnetic, while the Pr^{III} and Eu^{III} complexes are noninteracting. In these two reports, the exchange couplings involving the heavier lanthanides with more that seven f electrons did not match either the theoretical prediction in all cases or each other. Recently, Diaz et al. have studied the nature of the exchange interactions in the cyano-bridged dinuclear $Fe^{III}Ln^{III}$ complexes.[9c] These complexes, particularly the higher analogues, again do not follow any systematic trend. However, Kahn et al.[13] have demonstrated antiferromagnetic and ferromagnetic interactions between radicals and lanthanides with, respectively, $4f^1-4f^5$ and $4f^7-4f^{10}$ configurations. As discussed above, the metal centers in the $Cu^{II}Gd^{III}$, $Cu^{II}Tb^{III}$, $Cu^{II}Dy^{III}$, $Cu^{II}Ho^{III}$, $Cu^{II}Tm^{III}$, and $Cu^{II}Yb^{III}$ complexes are ferromagntically coupled. Among the lower members of the series, the Ce^{III}, Nd^{III}, and Sm^{III} complexes exhibit antiferromagnetic interactions, while the metal ions in the $Cu^{II}Pr^{III}$ and $Cu^{II}Eu^{III}$ complexes are noncorrelated. Thus, except for the Er^{III} complex, for which no definite conclusion could be drawn, the observations made in this study fairly agree with the proposition of Kahn.[5,9a] It is relevant to compare the nature of the magnetic interactions in complexes **3**−**14** with the couplings in the similar diphenoxo-bridged Schiff base compounds reported previously by Costes et al.[9b] As summarized in Table 5, the natures of the interactions are different only in the last three members. In contrast to the observed antiferromagnetism in the Tm^{III} and Yb^{III} complexes in the Costes report, the interaction in the $Cu^{II}Tm^{III}$ and $Cu^{II}Yb^{III}$ complexes reported here is ferromagnetic. Again, while they observed ferromagnetic interaction in the Er^{III} compound, no conclusion can be drawn regarding the interaction in the similar compound **12**.

Significant Aspects of the Complexes Reported Here. Since the magnetic orbitals in lanthanides are deep-seated, relatively weak exchange interactions are observed in their compounds. In the case of isotropic gadolinium(III) as one of the spin carriers, the maximum value reported for the ferromagnetic exchange integral ($\mathbf{H} = -2J\mathbf{S}_1\cdot\mathbf{S}_2$) is only 6.0 cm^{-1}.[4a] Due to the weak interactions in the Ln^{III} compounds, any significant increase or decrease of $\chi_M T$ (for Gd^{III}) or $\Delta\chi_M T$ (for other Ln^{III} metals) takes place below 50 K. Again, the values of $\chi_M T$ (for all Ln^{III} metals) and $\Delta\chi_M T$ (for Ln^{III} metals other than Gd^{III}) at 300 K of the exchange-coupled 3d−4f or 4f−radical systems have been found very close to the values expected for isolated systems.[1a,2−12]

Although some complexes reported here exhibit magnetic behavior similar to that of the known examples, the cryomagnetic properties of some others are quite unusual. Prior to the discussion of the unusual findings, it will be appropriate to consider Figure 13, where the calculated $\Delta\chi_M T$ ($\chi_M T(Cu^{II}Gd^{III}) - \chi_M T(Ni^{II}Gd^{III})$) versus T curves for the Gd^{III} systems with different J values ($\chi_M T$ of the $Ni^{II}Gd^{III}$ system has been fixed at 7.88 $cm^3\ mol^{-1}$ K throughout the temperature range) are shown. For the smaller J values, $\Delta\chi_M T$ at 300 K is very close to the expected value of the isolated spins and $\Delta\chi_M T$ remains almost constant in the temperature range 300−50 K. As the J value increases, $\Delta\chi_M T$ at 300 K deviates more and more and the temperature below which the rapid increase takes place becomes higher and higher. For $J = 1$ cm^{-1} and a hypothetical larger J value of 10 cm^{-1}, the $\Delta\chi_M T$ values at different temperatures are as follows [T (K), $\Delta\chi_M T$ ($cm^3\ mol^{-1}$ K) for $J = 1$ cm^{-1}, $\Delta\chi_M T$ ($cm^3\ mol^{-1}$ K) for $J = 10$ cm^{-1}]: 300, 0.391, 0.558; 250, 0.395, 0.595; 200, 0.401, 0.649; 150, 0.410, 0.737; 100, 0.429, 0.905; 75, 0.448, 1.062; 50, 0.485, 1.333; 25, 0.595, 1.834; 8, 1.024, 2.121; 5, 1.33, 2.123. From the above trend of the variation of $\Delta\chi_M T$ with T in terms of two different J values of a $Cu^{II}Gd^{III}$ system, it is possible to conclude qualitatively the relative strengths of exchange interactions in compounds containing other lanthanides by considering the following facts: deviation of the $\Delta\chi_M T$ values at 300 K, the trends of the profiles in the higher temperature range, the temperature below which the rapid increase (for the ferromagnetically coupled systems) takes place, and the maximum value of $\Delta\chi_M T$ at low temperatures.

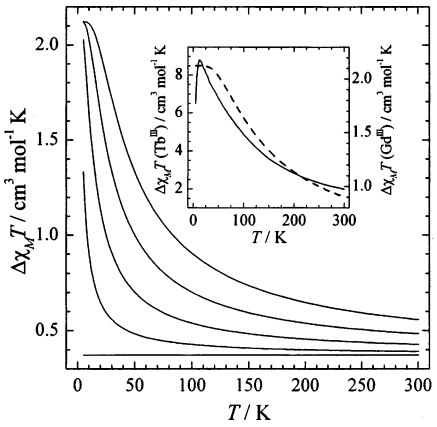

Figure 13. Temperature dependence of the theoretical $\Delta\chi_M T$ for the Cu^{II}-Gd^{III} system having different J values. The J values for the solid lines from bottom to top are 0, 1, 3, 6, and 10 cm^{-1}, respectively. Inset: the observed $\Delta\chi_M T$ (solid lines) for the Tb^{III} system has been compared with the theoretical $\Delta\chi_M T$ (dashed lines) of the $Cu^{II}Gd^{III}$ compound having a large and hypothetical J value, 30 cm^{-1}.

As mentioned earlier, the noninteracting nature of the Pr^{III} and Eu^{III} complexes **4** and **7** has been observed previously in the related diphenoxo-bridged compounds reported by Costes et al.[9b] The metal centers in three other lower members (**3**, **5**, and **6**) are antiferromagnetically coupled.

Similar observations have also been found by the Costes group.[9b] However, there are some significant differences; unlike the previous cases where $\Delta\chi_M T$ remains constant in the temperature range 300−50 K, $\Delta\chi_M T$ of the Ce^{III} and Nd^{III} compounds exhibits a slow but definite decrease in this temperature range. Evidently, the magnitude of the interactions in the complexes **3** and **5** is larger compared to that of the previously reported diphenoxo-bridged $Ce^{III}Ce^{III}$ and $Ce^{III}Nd^{III}$ compounds. For the Dy^{III} compound in the Costes report, $\Delta\chi_M T$ at 300 K is very close to 0.38 $cm^3\ mol^{-1}$ K and remains constant up to ca. 25 K. Below 25 K, $\Delta\chi_M T$ increases to ca. 2.5 $cm^3\ mol^{-1}$ K at 2 K. A similar observation was reported for the Tb^{III} compound. In contrast, the $\Delta\chi_M T$ values of the $Cu^{II}Tb^{III}$ compound **9** at 300, 250, 200, 150, 100, 75, 50, and 16 K are 1.99, 2.33, 2.84, 3.59, 4.82, 5.78, 6.79, and 8.71 $cm^3\ mol^{-1}$ K, respectively. Clearly, the paramagnetic centers in the $Cu^{II}Tb^{III}$ complex **9** are strongly coupled. Indeed, the extent of coupling is so strong that the $\Delta\chi_M T$ value at 300 K is much greater than the value expected for copper(II) only. In the inset of Figure 13, $\Delta\chi_M T$ of the Tb^{III} system has been compared with the theoretical $\Delta\chi_M T$ of the $Cu^{II}Gd^{III}$ system having a large J value of 30 cm^{-1}. The slopes of the curves in the two cases are similar. It should be noted, however, that the scales of the two $\Delta\chi_M T$ axes in the inset of Figure 13 are different and there should be no relation between the absolute values of the exchange interactions in the two cases. Moreover, the hypothetical J value of 30 cm^{-1} in a $Cu^{II}Gd^{III}$ compound seems to be an impossibility. Nevertheless, on the basis of the similarities in the slopes of the two curves (in the inset of Figure 13), it can be argued that the ferromagnetic interaction in the $Cu^{II}Tb^{III}$ compound **9** is significantly strong. If the $\Delta\chi_M T$ versus T data, as discussed in ref 9b, of the Tb^{III} system derived from H_2L^2 are plotted in the same scale range as in the inset of Figure 13, a practically horizontal line will be obtained. Evidently, the $Cu^{II}Tb^{III}$ compound **9** exhibits a much stronger ferromagnetic interaction than the interaction observed in the similar system derived from H_2L^2. For the Dy^{III} system, although the increase is very rapid only below 25 K, $\Delta\chi_M T$ increases significantly (from 1.43 to 3.56 $cm^3\ mol^{-1}$ K) in the temperature range 300−50 K. Moreover, the magnitude of the $\Delta\chi_M T$ value (13.52 $cm^3\ mol^{-1}$ K) at 5 K indicates that here also the ferromagnetic interaction is appreciably strong. The higher $\Delta\chi_M T$ values at 300 K as well as the significant increase of $\Delta\chi_M T$ throughout the temperature range are indicative of strong interactions in the Tm^{III} and Yb^{III} compounds. In the case of the Ho^{III} complex, the large magnitude of $\Delta\chi_M T$ at 5 K may be considered as an indication of appreciable ferromagnetic coupling between copper(II) and holmium(III).

It is a generally accepted concept that the interactions between 4f and 3d ions or radicals will be weak and will be perceptible only at low temperatures (ca. below 50 K). However, for the $Cu^{II}Gd^{III}$ compounds with J = ca. 5 cm^{-1} and for a few of the radical−Ln^{III}−radical compounds,[13] we note a somewhat higher interaction. As an example, the $\Delta\chi_M T$ values of the Dy^{III} system, reported therein, at 300, 250, 200, 150, 100, 75, 50, and 8 K are, respectively, ca. 0.8 (equivalent to two noncorrelated local doublets), 0.9, 1.05, 1.24, 1.55, 1.80, 2.28, and 4.82 $cm^3\ mol^{-1}$ K. These values indicate that, although the rapid increase of $\Delta\chi_M T$ takes place below 50 K, there is a definite increase of $\Delta\chi_M T$ in the temperature range 300−50 K. In contrast, in most of the cases including the previous report of the diphenoxo-bridged systems, $\Delta\chi_M T$ remains practically constant in the temperature range 300−50 K (or 100 K). In the case of the above-mentioned Dy^{III}-radical system or some of the strongly coupled Gd^{III}-containing compounds (with J values around 5 cm^{-1}), the increase of $\chi_M T$ or $\Delta\chi_M T$ in the 300−50 K (or 100 K) temperature range is also not very significant. In addition, $\chi_M T$ or $\Delta\chi_M T$ at 300 K deviates only little from the value of the isolated system in the reported examples. All these are indicative of only a weak interaction in the lanthanide systems; some are only relatively a little more strongly coupled. Evidently, the stronger magnetic interactions observed in most of the compounds reported in this study are quite remarkable.

Reason for the Unusually Strong Magnetic Exchange Interactions. For the diphenoxo-bridged $Cu^{II}Gd^{III}$ complexes, Kahn[5] suggested that the magnitude of J should be a function of the dihedral angle (δ) between the CuO_2 and GdO_2 planes. The $Cu^{II}Ln^{III}$ complexes **27**−**38** (Ln = Ce − Yb) for which Costes et al. analyzed the exchange interactions were derived from the Schiff base ligand H_2L^2.[9b,11a] The dihedral angles in these complexes **27**−**38** are fairly larger (e.g., the δ values in the $Cu^{II}Ce^{III}$ and $Cu^{II}Yb^{III}$ complexes are 14.3° and 13.2°, respectively)[9b] as compared to those of the related compounds reported here (e.g., the δ values in the $Cu^{II}Ce^{III}$ and $Cu^{II}Yb^{III}$ complexes are 3.5° and 4.3°, respectively). Evidently, the magnetic exchange interaction in **27**−**38** should be weaker relative to that in **3**−**14**. The dihedral angles and the exchange integrals in the $Cu^{II}Gd^{III}$ complexes **8**[4b] (δ = 4.3°, J = 4.04 cm^{-1}) and **32**[11a] (δ = 12.9°, J = 3.5 cm^{-1}) are in agreement with this expectation. Clearly, the strong exchange interactions reported in this study must be related to the smaller dihedral angles between the CuO_2 and LnO_2 planes. It also appears that the effect of the dihedral angle is more prominent in the case of the higher lanthanides.

Conclusions

The syntheses, characterization including structure determinations of 13 compounds, and magnetic properties of the series of isostructural $Cu^{II}Ln^{III}$ and $Ni^{II}Ln^{III}$ complexes $[M^{II}L^1Ln^{III}(NO_3)_3]$ (M = Cu or Ni; Ln = Ce − Yb) with the hexadentate Schiff base compartmental ligand *N*,*N*′-ethylenebis(3-ethoxysalicylaldiimine) (H_2L^1) have been described in this paper. The metal centers in the $Cu^{II}Gd^{III}$ compound in this series are ferromegnetically coupled.[4b] The nature of the exchange interactions in other $Cu^{II}Ln^{III}$ systems has been inferred from the $\Delta\chi_M T$ versus T plots, where $\Delta\chi_M T$ is the difference between the values of $\chi_M T$ for the $Cu^{II}Ln^{III}$ and corresponding $Ni^{II}Ln^{III}$ systems. Ferromagnetic interactions seem to be exhibited by the $Cu^{II}Tb^{III}$, $Cu^{II}Dy^{III}$, $Cu^{II}Ho^{III}$, $Cu^{II}Tm^{III}$, and $Cu^{II}Yb^{III}$ complexes, while, for the $Cu^{II}Er^{III}$ system, no definite conclusion could be reached. On the other hand, among the lower members of the series,

the complexes of Ce^{III}, Nd^{III}, and Sm^{III} exhibit antiferromagnetic interactions, while the $Cu^{II}Pr^{III}$ and $Cu^{II}Eu^{III}$ complexes behave as spin-uncorrelated systems. A qualitative model has been proposed here to understand the relative strengths of the exchange interactions in systems containing anisotropic lanthanides. On the basis of this model, the exchange interactions in the interacting $Cu^{II}Ln^{III}$ compounds, particularly in the higher analogues, have been concluded as significantly strong, which can be rationalized in terms of the planarity of the bridging moieties.

Acknowledgment. Financial support from the Department of Science and Technology, Government of India (Grant SR/S1/IC-27/2002), and the National Science Council, Taiwan (Grant NSC93-2113-M032-002), is gratefully acknowledged. H.-H.W. is thankful to G.-H. Lee of the Instrumental Center, National Taiwan University, Taiwan, for data collection and solution of the structure of **10**. S.M. thanks Dr. G. Mostafa, Department of Physics, Jadavpur University, India, for helpful discussion regarding the refinement of the structure of **14**. S.M. is also grateful to the reviewers of the manuscript for their valuable suggestions.

Supporting Information Available: Crystallographic data in CIF format for the 13 complexes, and Table S1 and Figures S1−S7 (PDF). This material is available free of charge via the Internet at http://pubs.acs.org.

IC048196H